

BBABIO 43850

## Kinetic characterization of the reconstituted dicarboxylate carrier from mitochondria: a four-binding-site sequential transport system

C. Indiveri<sup>a</sup>, G. Prezioso<sup>a</sup>, T. Dierks<sup>b</sup>, R. Kramer<sup>b</sup> and F. Palmieri<sup>a</sup>

<sup>a</sup> Department of Pharmaco-Biology, Laboratory of Biochemistry and Molecular Biology, University of Bari and CNR Unit for the Study of Mitochondria and Bioenergetics, Bari (Italy) and <sup>b</sup> Institut für Biotechnologie, Forschungszentrum Jülich, Jülich (Germany)

(Received 26 November 1992)

**Key words** Reconstitution, Dicarboxylate carrier, Transport mechanism, (Rat liver mitochondria)

The mitochondrial antiport carriers form a protein family with respect to their structure and function. The kinetic antiport mechanism, being of the sequential type, shows that the dicarboxylate carrier also belongs to this family. This was demonstrated by bireactant initial velocity studies of the purified and reconstituted carrier protein. The transport affinity of the carrier for the internal substrate was largely independent of the external substrate concentration and vice versa, whereas the carrier's apparent  $V_{\max}$  rose with increasing saturation of internal and external binding sites. Thus, the carrier forms a catalytic ternary complex with one internal and one external substrate molecule. As compared to other mitochondrial antiport carriers, however, the situation with the dicarboxylate carrier is more complex. On each membrane side of the protein two separate binding sites exist, one specific for phosphate (or its analogue phenyl phosphate), the other specific for dicarboxylate (or butyl malonate), that can be occupied by the respective substrates without mutual interference. This became evident from the non-competitive interaction of these substrates (or analogues) with the carrier. The two external, but not the two internal binding sites could be saturated simultaneously with phosphate and malate, thereby causing inhibition of transport. All four binding sites must be associated with the same translocation pathway through the carrier protein, since the sequential antiport mechanism held true for the phosphate/malate heteroexchange as well as for the malate/malate or phosphate/phosphate homoexchange.

### Introduction

The dicarboxylate carrier of liver mitochondria plays an important role in gluconeogenesis, urea synthesis and sulphur metabolism (for reviews see Refs. 1 and 2). This carrier catalyzes an electroneutral exchange of certain dicarboxylates (e.g., malate, succinate) for inorganic phosphate [3–8]. Inorganic sulphur-containing compounds (e.g., sulphate, thiosulphate) are also translocated by this transport system [9,10].

With respect to function, the dicarboxylate carrier is a unique transport system. It translocates chemically different substrates and, moreover, translocation involves two separate binding sites present at the cytosolic side and, as will be shown here, also at the matrix side of the carrier protein. One binding site is specific for phosphate and thiosulphate, the other for dicarboxylates, sulphate and sulphite.

For the cytosolic membrane surface this was suggested by early studies in intact mitochondria [7,11,12] and, after we had purified [13] and reconstituted the carrier protein [13,14], was demonstrated in a proteoliposomal system [15].

The functional reconstitution of the isolated protein allowed us to gain an insight into the relatively complex kinetic behavior of this carrier resulting from the presence of two distinct binding sites at either membrane surface. For the external side of the proteoliposomes, evidence was obtained that both binding sites could be saturated simultaneously with malate and phosphate, respectively, leading to the formation of a non-catalytic ternary complex with the carrier molecule [15]. In the present paper we have investigated the reconstituted carrier protein with respect to the internal side and the kinetic mechanism underlying counterexchange of one internal and one external substrate molecule. Previous studies of mitochondrial antiport carriers have established a common functional model including as the catalytic intermediate a ternary carrier complex with one substrate molecule bound from each side of the membrane [16–21]. In this respect, the finding that the

Correspondence to: F. Palmieri, Dipartimento Farmaco-Biologico, Università di Bari, Traversa 200 Re David, 4, 70125 Bari, Italy.  
Abbreviations: Pipes, 1,4-piperazinediethanesulphonic acid, SDS, sodium dodecyl sulphate.

dicarboxylate carrier bears two distinct substrate binding sites at its external surface [7,15] and, as will be shown here, also at the internal side was a challenge to the general carrier concept. Therefore, it was our main interest to clarify, how the different binding sites participate in the antiport mechanism in a concerted manner.

## Materials and Methods

**Materials** Hydroxyapatite (Bio-Gel HTP) and Dowex AG1-X8 were purchased from Bio-Rad, Amberlite XAD-2 from Fluka, Sephadex G-75 from Pharmacia, [ $^{32}\text{P}$ ]phosphate and L-[U- $^{14}\text{C}$ ]malate from Amersham, egg-yolk phospholipids (L- $\alpha$ -phosphatidylcholine from fresh turkey egg yolk), Pipes (1,4-piperazinediethanesulphonic acid) and Triton X-114 from Sigma. All other reagents were of analytical grade.

**Isolation of the dicarboxylate carrier** The dicarboxylate carrier was purified from rat liver mitochondria by the Amberlite/hydroxyapatite procedure as described previously [13]. The purity of the 28 kDa band protein previously identified as the dicarboxylate carrier [13] was always higher than 95% as checked by SDS-polyacrylamide gel electrophoresis. Furthermore, the purified dicarboxylate carrier was not contaminated by known mitochondrial transport systems such as the ADP/ATP carrier and the phosphate carrier.

**Reconstitution of the dicarboxylate carrier** The purified dicarboxylate carrier was passed through a Dowex AG1-X8 column, 100–200 mesh, chloride form ( $0.5 \times 8$  cm) equilibrated with a buffer containing 10 mM Pipes (pH 7.0) and 1 mg/ml egg-yolk phospholipids in the form of sonicated liposomes, in order to remove the interfering anions such as phosphate from the hydroxyapatite and sulphate from the solubilization buffer (see Ref. [13]). Liposomes were prepared as described previously [22] by sonication of 100 mg/ml egg-yolk phospholipids in water for 60 min. Reconstitution of the dicarboxylate carrier into liposomes was performed by removing the detergent with Amberlite [23] from mixed micelles containing detergent, protein and phospholipids. The composition of the mixture used for reconstitution was 200  $\mu\text{l}$  of the purified dicarboxylate carrier (7–15  $\mu\text{g}$  protein), 60  $\mu\text{l}$  of 10% Triton X-114, 6.7 mg of phospholipids in the form of sonicated liposomes, phosphate or malate at the indicated concentrations, 10 mM Pipes (pH 7) in a final volume of 0.68 ml. After vortexing, this mixture was passed 13 times through the same Amberlite column ( $0.5 \times 3.2$  cm) pre-equilibrated with a buffer containing 10 mM Pipes and the same concentration of the substrate present in the starting mixture. All the operations were performed at 4°C except the passages through Amberlite, which were carried out at room temperature.

**Transport measurements** In order to remove the

external substrate, the proteoliposomes were passed through a Sephadex G-75 column ( $0.7 \times 15$  cm) pre-equilibrated with 10 mM Pipes (pH 7) and an appropriate concentration of NaCl to balance the internal osmolarity. The transport activity was determined by measuring the flux of labelled substrates from outside to inside (forward exchange) or from inside to outside (backward exchange) [24]. For backward-exchange measurements, the internal substrate pool of the proteoliposomes was labelled by carrier-mediated equilibration with 0.5  $\mu\text{M}$  [ $^{32}\text{P}$ ]phosphate or [ $^{14}\text{C}$ ]malate added at high specific radioactivity whereby the internal substrate concentration was not changed (homoeexchange conditions). After 30 minutes, the radioactivity not taken up was removed by passing the proteoliposomes again through Sephadex G-75 (see above). The transport measurement was started, in the case of the backward exchange, by adding unlabelled substrate to the proteoliposomes or, in the case of the forward exchange, by adding labelled substrate at the indicated concentrations. In either method, the exchange was stopped by addition of 20 mM butyl malonate and 20 mM pyridoxal 5-phosphate. In control samples the inhibitors were added at time zero according to the inhibitor stop method [24]. The assay temperature was 25°C. Finally, each sample of proteoliposomes (100  $\mu\text{l}$ ) was applied on an anion-exchange column (Dowex AG1-X8, acetate form,  $0.5 \times 5$  cm) in order to separate the external label from the radioactivity remaining inside. The liposomes were eluted with 40 mM sodium acetate directly into the scintillation liquid.

The isotope equilibration between the external and the internal compartment was followed by stopping the exchange after different time intervals. In the case of forward-exchange determinations, the transport rate usually was calculated from the radioactivity taken up by the proteoliposomes within 60 s. It was important for heteroexchange experiments to stay as close as possible to initial conditions in order to avoid interference of the transported substrate in the opposite compartment. Faster kinetics, which were not linear for the first minute, were fitted by a computer program according to a first-order process equation allowing calculation of the initial transport rate, which is expressed as  $\mu\text{mol}/\text{min}$  per mg protein. In the case of backward-exchange determinations, the decrease of radioactivity inside the liposomes until equilibrium was fitted according to a single exponential decay equation, from which the first-order rate constant,  $k$ , was derived. The backward-exchange rates were calculated as the product of  $k$  and the substrate concentration inside the liposomes, as described previously [19].  $K_m$  and  $V_{\text{max}}$  values were determined by a computer-fitting program based on linear regression analysis.

**Other methods** The protein concentration was determined by the Lowry method modified for the pres-

TABLE I

*K<sub>m</sub> values of the reconstituted dicarboxylate carrier*

Transport affinities were determined by the forward and by the backward exchange method (see Materials and Methods). The values are means  $\pm$  SE (*n*) n.d., not determined

Substrate	Membrane side	Counter substrate	<i>K<sub>m</sub></i> (mM)	
			forward exchange	backward exchange
Malate	external	malate	0.49 $\pm$ 0.05 <sup>a</sup>	0.41 $\pm$ 0.16 (3)
	external	phosphate	0.5	n.d.
	internal	malate	0.92 $\pm$ 0.24 (8)	0.92 $\pm$ 0.16 (3)
	internal	phosphate	0.83 $\pm$ 0.20 (5)	0.93 $\pm$ 0.18 (3)
Phosphate	external	malate	1.41 $\pm$ 0.35 <sup>a</sup>	1.0
	external	phosphate	1.4	n.d.
	internal	malate	0.84 $\pm$ 0.19 (8)	0.90
	internal	phosphate	0.89 $\pm$ 0.25 (4)	0.90 $\pm$ 0.30 (4)

<sup>a</sup> From Ref. 18

ence of Triton [25]. SDS polyacrylamide slab-gel electrophoresis of acetone-precipitated samples and staining with silver nitrate were performed as described previously [26]. The activity of other transport systems was assayed by the inhibitor stop method [24] using the following stop inhibitors: *N*-ethylmaleimide (phosphate carrier), 1,2,3-benzenetricarboxylate (citrate carrier), phthalonate (2-oxoglutarate carrier), carboxyatractylolide (ADP/ATP carrier), pyridoxal phosphate (aspartate/glutamate carrier),  $\alpha$ -cyanocinnamate (pyruvate carrier), *N*-ethylmaleimide (carnitine carrier) and mersalyl (ornithine carrier).

## Results

### Kinetic description of the internal substrate binding sites

At the external membrane surface of the reconstituted dicarboxylate carrier two distinct and specific

binding sites were characterized previously (see Introduction). The transport affinities referring to the dicarboxylate (*K<sub>m</sub>* 0.5 mM) and the phosphate site (*K<sub>m</sub>* 1.4 mM) are given in Table I. In order to describe the internal binding site(s) of the reconstituted protein we applied two different methods measuring either the flux of labelled substrate from outside to inside (forward exchange) or from inside to outside (backward exchange), respectively (see Materials and Methods). Only the latter technique allows us to measure antiport activity even at relatively low internal substrate concentrations (< 200  $\mu$ M), as was explained earlier [19]. Both modes of analysis led to coincident results, as was checked in particular by determining the *K<sub>m</sub>* for external malate yielding values of 0.49  $\pm$  0.05 mM (forward exchange) or 0.41  $\pm$  0.16 mM (backward exchange), respectively (Table I).

The determination of the internal kinetic constants

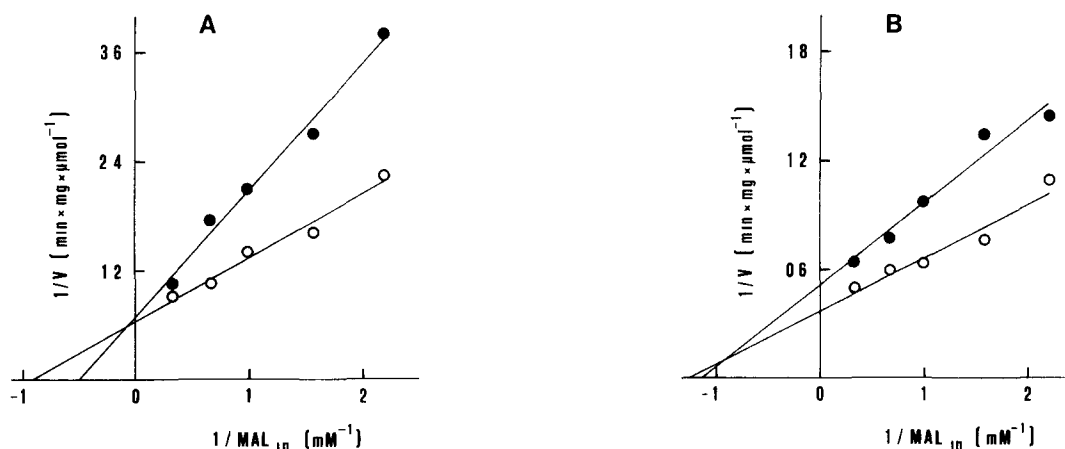


Fig. 1 Inhibition of malate/malate homoexchange by intraliposomal butyl malonate and phenyl phosphate. Proteoliposomes contained malate at the indicated concentrations with (●) and without (○) 0.6 mM butyl malonate (A) or 2 mM phenyl phosphate (B). The transport was measured by the forward exchange technique (see Materials and Methods) after addition of 0.1 mM labeled malate. The *K<sub>m</sub>* value for internal malate was 1.1 mM (A) or 0.81 mM (B), respectively. The *K<sub>i</sub>* for internal butyl malonate was 0.69 mM, for internal phenyl phosphate 2.4 mM.

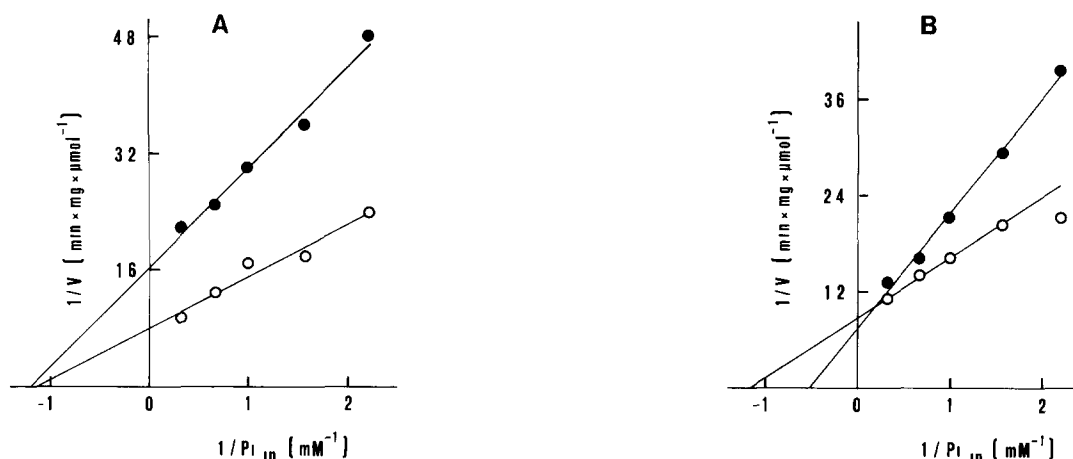


Fig 2 Inhibition of malate/phosphate heteroexchange by intraliposomal phenyl phosphate and butyl malonate. Proteoliposomes contained phosphate at the indicated concentrations with (●) and without (○) 0.6 mM butyl malonate (A) or 2 mM phenyl phosphate (B). The transport was measured by the forward exchange technique (see Materials and Methods) after addition of 0.1 mM labeled malate. The  $K_m$  value for internal phosphate was 0.88 mM (A) or 0.85 mM (B), respectively. The  $K_i$  for internal butyl malonate was 0.57 mM, for internal phenyl phosphate 1.6 mM.

requires many preparations of proteoliposomes with different internal substrate concentrations. Therefore the results to be obtained were in principle not as precise as those referring to the external membrane side. The backward exchange method led to internal  $K_m$  values that were rather similar for both phosphate and malate (about 0.9 mM). This concentration range could be investigated also in the forward exchange mode yielding  $K_m$  values of  $0.92 \pm 0.24$  mM for malate and  $0.84 \pm 0.19$  mM for phosphate (Table I). These values obtained by multiple determinations were independent of the nature of the (external) countersubstrate (malate or phosphate, respectively), an equivalent independence was observed when determining the external transport affinities (Table I).

In order to find out whether two binding sites can be distinguished at the internal surface similar to those

we observed outside, we investigated the mutual interaction of dicarboxylates and phosphate with the carrier protein at its internal surface. For these experiments we applied the substrate analogues butyl malonate and phenyl phosphate which, on the outside, interacted specifically only at the dicarboxylate or phosphate site, respectively, without being transported [15,27]. The Lineweaver-Burk plots of Fig 1 show the inhibition of malate (external)/malate (internal) exchange by the presence of internal butyl malonate (0.6 mM) or internal phenyl phosphate (2 mM). In the case of butyl malonate a competitive inhibition was observed (Fig 1A), whereas phenyl phosphate inhibited non-competitively (Fig 1B), i.e., only phenyl phosphate gave rise to a significant reduction of  $V_{max}$ . Just the opposite result was obtained when investigating the exchange of malate (external)/phosphate (internal). The presence of inter-

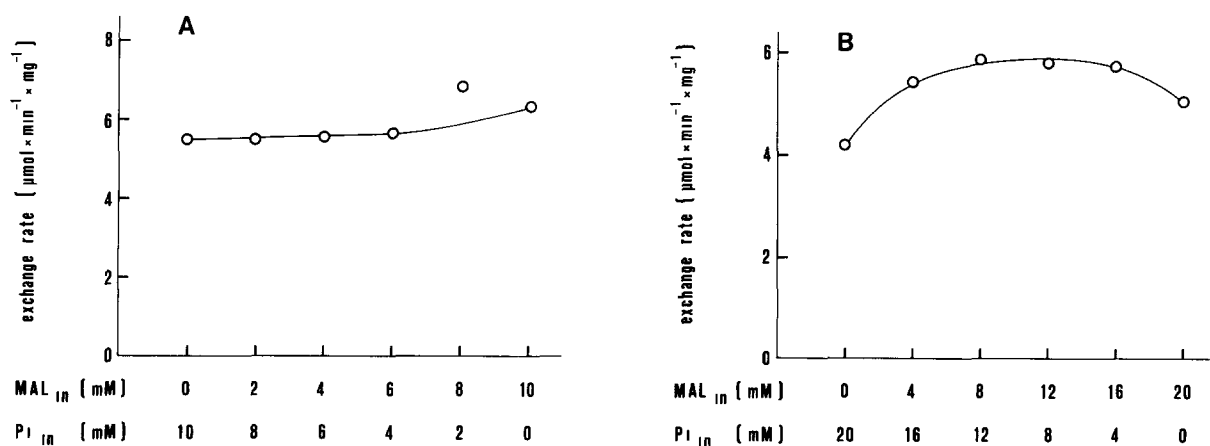


Fig 3 Dependence of exchange activity on the concentration of malate and phosphate present together inside the proteoliposomes. The proteoliposomes were loaded with different combinations of malate and phosphate, as indicated, at a total concentration of 10 mM (A) or 20 mM (B). Exchange was measured as uptake of 2 mM labeled malate.

nal butyl malonate led to a non-competitive kinetic pattern, internal phenyl phosphate inhibited in a competitive manner (Fig 2) Non-specific effects of butyl malonate or phenyl phosphate at the applied concentrations on liposome integrity could be ruled out (data not shown) These results demonstrate that at the internal membrane surface also two different binding sites can be distinguished, one specific for dicarboxylates and the other specific for phosphate Both sites show similar half-saturation constants ( $K_m$  0.9 mM) that are intermediate between the  $K_m$  for external malate (0.5 mM) and the  $K_m$  for external phosphate (1.4 mM)

A particular kinetic property of the dicarboxylate carrier observed at its external side [7,15] was tested for the internal compartment of the proteoliposomes, namely, the occurrence of a non-catalytic carrier complex when both binding sites were occupied simultaneously by the respective substrates This inactive complex was documented by a reduced turnover of the carrier when, externally, malate and phosphate were present at a 1:1 ratio, both at nearly saturating concentration [15] This was tested for the internal compartment as follows: if the sum of malate and phosphate concentration was constant (10 mM), but the portion contributed by the two substrates was varied (0–10 mM), then a minimum transport at about 5 mM concentration of each substrate would be expected However, this was not the case, neither at 2 mM (Fig 3A) nor at 0.1 mM external malate (not shown) Obviously, a non-translocating carrier complex is not formed because, upon binding of the first substrate, the transport event takes place before the second binding site also is occupied (see Discussion) Only non-transported ligands like butyl malonate or phenyl phosphate will lead to an inactive carrier, as observed in Figs 1B and 2A

Surprisingly, when the experiment of Fig 3A was carried out at a total malate plus phosphate concentration of 20 mM (Fig 3B) or 30 mM (not shown), an activity maximum corresponding to the carrier's  $V_{max}$  (see Figs 1 and 2) was observed at concentration ratios malate/phosphate of 1:4 to 4:1 However, if solely malate or phosphate (20–30 mM) was present inside the liposomes, the carrier was significantly inhibited (Fig 3B) This inhibition by high substrate concentrations (above 10–15 mM) more directly is demonstrated in Fig 4A However, raising the concentration of either substrate to this range had no such effect, if both malate and phosphate were present simultaneously inside the liposomes (Fig 4B) Even when choosing a scale on the abscissa with respect to only one substrate concentration (phosphate in Fig 4C), the positive effect of the other substrate on carrier activity became obvious Osmotic or salt effects as a possible reason for carrier inhibition could definitely be excluded, e.g., by

control liposomes containing 10 mM malate or phosphate plus 0–50 mM NaCl (Fig 4A) Thus, internally an inhibition may result if, at high substrate concentra-

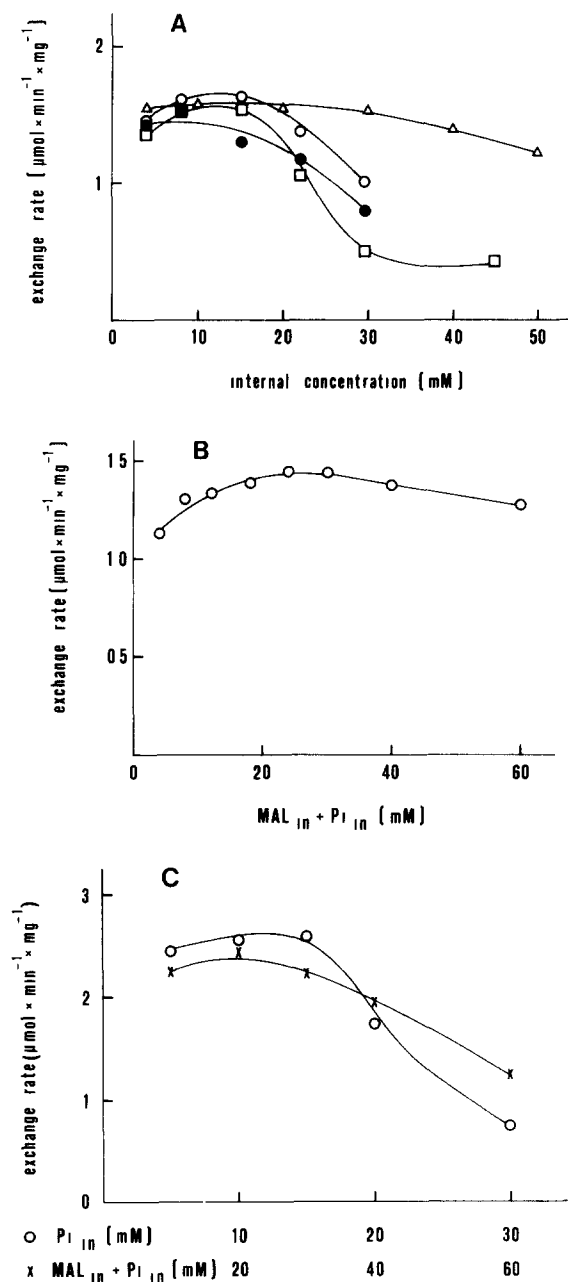


Fig 4 Dependence of exchange activity on the concentration of dicarboxylate and phosphate present separately (A and C) or together (B and C) inside the proteoliposomes (A) Proteoliposomes were loaded with the indicated concentrations of malate (○), malonate (●) phosphate (□) or NaCl (Δ), in the latter case additionally a fixed concentration (13 mM) of phosphate was loaded with NaCl (B) Proteoliposomes were loaded with equimolar malate and phosphate at the total concentrations indicated (C) Proteoliposomes were loaded with phosphate alone (○) or with malate and phosphate together (×) at the indicated concentrations In all experiments exchange was measured as uptake of 0.1 mM labeled malate Note that all data shown in panel C were obtained in a single experiment from parallel samples (○, ×)

tion, phosphate binds not only to the phosphate but also to the dicarboxylate site or if, vice versa, malate also binds to the phosphate site (see Discussion). It has to be pointed out that in a concentration range up to 10 mM there was no such interference, so that Michaelian kinetics were observed, a prerequisite for a reliable analysis of the antiport mechanism

#### Kinetic transport mechanism

The counterexchange of substrates catalyzed by an antiport carrier can be described in terms of a two-substrate reaction involving different association/dissociation and catalytic steps. The sequence of these steps follows one of two basically different bireactant mechanisms, the ping-pong or the sequential type [28]. In order to find out which of the two mechanisms applies to the reconstituted dicarboxylate carrier the antiport

reaction had to be analyzed varying in a single experiment both external and internal substrate concentrations in the  $K_m$  range. The results of such a bireactant initial velocity study of the malate/phosphate heteroexchange are given in Fig 5. Lineweaver-Burk plots show the dependence of antiport velocity on external malate (0.1–1 mM) at four different internal phosphate concentrations (0.5–5 mM). This analysis led to a kinetic pattern of straight lines converging close to the abscissa axis (Fig 5A). A similar result was obtained when plotting the same data as a function of the internal phosphate concentration (Fig 5C). This intersecting pattern demonstrates that the antiport reaction follows a sequential type of mechanism [28,29], implying that both countersubstrate molecules have to form a ternary complex with the carrier protein prior to the catalytic step (translocation). The transport rate was

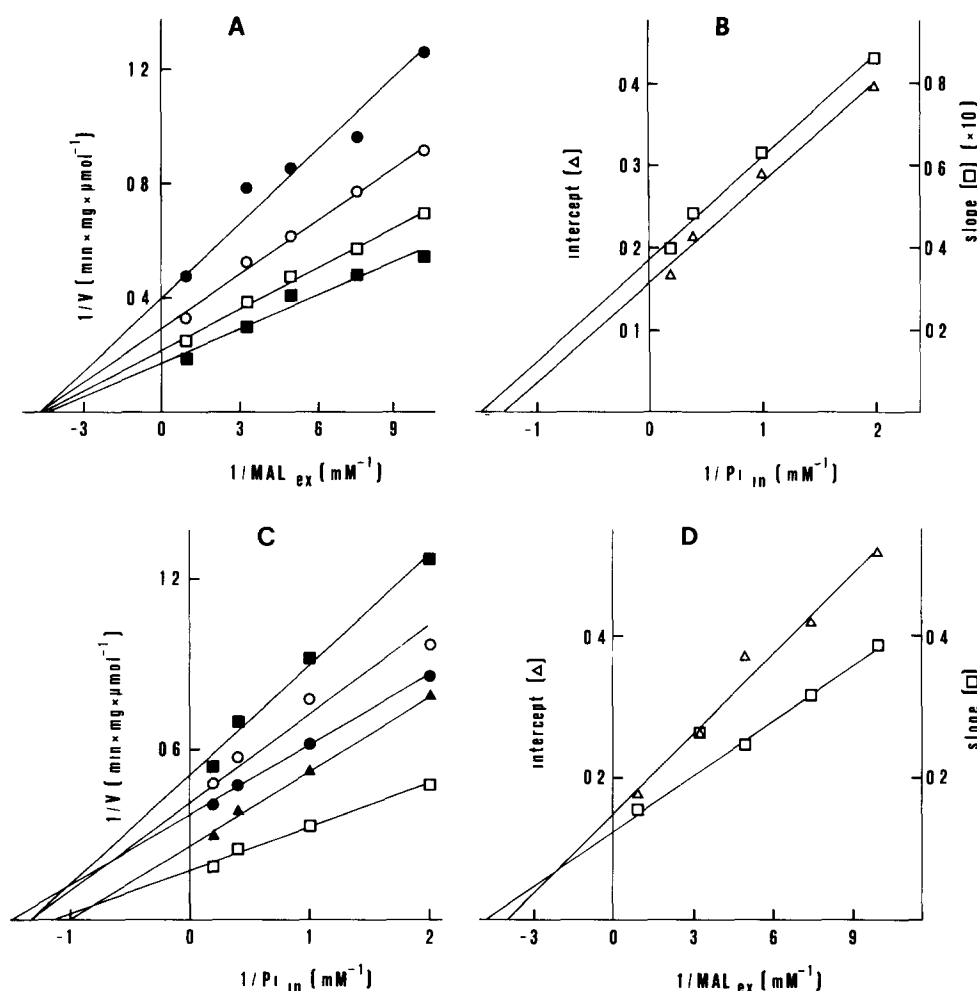


Fig 5 Bireactant initial velocity study of the malate/phosphate heteroexchange reaction catalyzed by the reconstituted dicarboxylate carrier (A, C) Lineweaver-Burk plots showing the dependence of exchange activity on external malate or internal phosphate, respectively. The concentrations of the countersubstrates were as follows (A) 0.5 (●), 1.0 (○), 2.5 (□) and 5.0 (■) mM internal phosphate (C) 0.10 (■), 0.13 (○), 0.20 (●), 0.30 (▲) and 1.0 mM (□) external malate. Exchange was measured by the forward exchange method. Initial rates were determined from the isotope equilibration curve with the help of a computer fitting program (see Materials and Methods). (B, D) Slope (□) and intercept (Δ) replots of primary plots A and C, respectively. The concentration-independent  $K_m$  values and  $K_i$  values (see text) were derived from B and D.  $K_m$  (external malate) 0.23 mM (B) and 0.27 mM (D),  $K_m$  (internal phosphate) 0.79 mM (B) and 0.89 mM (D),  $K_i$  (external malate) 0.20 mM (B),  $K_i$  (internal phosphate) 0.72 mM (D). The  $V_{max}$  was 6.4 (B) and 6.7  $\mu$ mol/min per mg protein.

stimulated mainly when raising the internal or external substrate concentration, as can be recognized from the effect on the apparent  $V_{\max}$  (ordinate intercept and slope effect). On the other hand, variation of the substrate concentration in one compartment only influenced to some extent the apparent transport affinity for the respective countersubstrate in the other compartment (reciprocal abscissa intercept). Thus, the binding of the internal and external substrate occurred largely independently of each other.

These interrelations could be quantitatively analyzed in secondary plots of the slopes and ordinate intercepts of Figs 5A and C vs the reciprocal concentration of the respective opposite substrate, as was carried out in Figs 5B and D, respectively. The linear relations obtained allowed us to extrapolate  $K_m$  values which were independent of the concentration of the respective countersubstrate (cf Ref. 28). These concentration-independent  $K_m$  values, namely 0.79–0.89 mM for internal phosphate and 0.23–0.27 mM for external malate, were very similar to those values determined at finite substrate concentration (Table I). Furthermore, the  $K_i$  values representing the dissociation constants of the binary carrier-substrate complexes, were derived from the replots. These  $K_i$  constants have a finite value only in case of a sequential mechanism [17]. Independent calculations from Fig. 5B for external malate ( $K_i$  0.20 mM) and from Fig. 5D for internal phosphate ( $K_i$  0.72 mM) led to values that were slightly lower than the respective  $K_m$  values. The

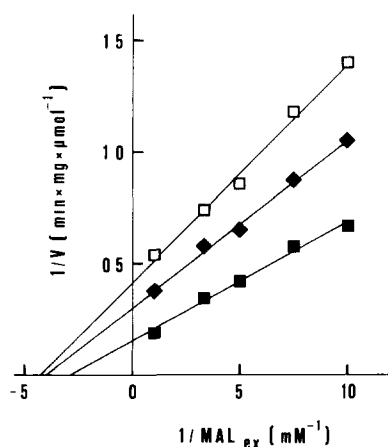


Fig. 6 Bireactant initial velocity study of the malate/malate homoexchange reaction catalyzed by the reconstituted dicarboxylate carrier. The Lineweaver-Burk plot shows the dependence of exchange activity on external malate at three different internal malate concentrations: 0.5 (□), 1.0 (◆) and 5.0 mM (■). Exchange rates were determined as described in Fig. 5. Concentration-independent  $K_m$  values and  $K_i$  values (see text) were derived from slope and intercept replots (not shown) in the same way as in Fig. 5.  $K_m$  (external malate) 0.37 mM,  $K_m$  (internal malate) 1.1 mM,  $K_i$  (external malate) 0.16 mM,  $K_i$  (internal malate) 0.48 mM. The  $V_{\max}$  was 7.3  $\mu\text{mol}/\text{min}$  per mg protein. All these values were the same whether determined on the basis of the primary curves shown (abscissa  $1/\text{external malate}$ ) or from the plot  $1/V$  vs  $1/\text{internal malate}$  (not shown).

$K_m/K_i$  ratio of about 1.2 for both external malate and internal phosphate is in agreement with sequential bisubstrate kinetics.

In view of two different binding sites involved in the transport of malate and phosphate it was important to find out whether the homoexchange also, like the heteroexchange, follows the sequential mechanism. Indeed the same basic type of kinetic mechanism was observed, when measuring malate/malate antiport (Fig. 6) or phosphate/phosphate antiport (data not shown). Moreover, for the malate/phosphate heteroexchange the result was independent of malate present externally (Fig. 5) or internally (not shown). Taken together, all kinetic patterns obtained at different substrate distributions were of the same, i.e., intersecting, type and the point of intersection usually was located close to the abscissa axis. The  $K_m/K_i$  ratios in all experiments were constant when determined independently for the internal or external substrate, respectively. However, this ratio sometimes was clearly higher than 1 (Fig. 6  $K_m/K_i$  2.3 for both external and internal malate). Despite these variations, which are difficult to explain, all data shown are in agreement with a rapid-equilibrium-random mechanism operative in the reconstituted dicarboxylate carrier.

## Discussion

### *The sequential transport mechanism – variations on a theme*

While on the internal side of the purified and reconstituted dicarboxylate carrier no significant difference in the transport affinity for malate and phosphate could be found ( $K_m \approx 0.9$  mM), externally the affinity for malate was clearly higher ( $K_m$  0.3–0.5 mM) than for phosphate ( $K_m$  1.4 mM). These  $K_m$  values were independent of each other, whether determined in homo- or heteroexchange experiments, i.e., with malate or phosphate on the opposite side of the membrane (Table I). Moreover, the  $K_m$  values also were largely independent of the concentration of this countersubstrate as became evident from two-reactant analyses (Figs 5 and 6). Major  $V_{\max}$  but minor  $K_m$  effects (on one membrane side), were observed, when varying the substrate concentration on the other membrane side. This predicts a reversible connection between the association steps of the internal and external substrate molecule with the carrier. A catalytic ternary complex is thereby formed that is translocation competent, hence indicating that the dicarboxylate carrier follows a sequential antiport mechanism. As observed in the case of other mitochondrial antiport carriers [16–21], a rapid-equilibrium random mechanism is most probable. This specific type of a sequential mechanism implies fast and independent binding of the two substrate molecules in random order. In line with this mecha-

nism, substrate binding to the free or to the single-occupied dicarboxylate carrier, as characterized by  $K_i$  and  $K_m$  values, respectively (see Results), occurred with similar affinity. In any case the ratio  $K_m/K_i$  for the external substrate was the same as for the internal substrate. However, a definite decision whether a random or an ordered type of a sequential mechanism is operative cannot be made, since in carrier kinetics product inhibition studies cannot be performed.

In the family of sequential mitochondrial carriers the dicarboxylate carrier certainly is extraordinary: on each membrane side there is not only one binding site that can be occupied by both countersubstrate species, but two binding sites with distinct specificity which take part in translocation. Dicarboxylate and phosphate are structurally less related than the substrates of the aspartate/glutamate, oxoglutarate/malate or ADP/ATP carrier, possibly in this way their transport can be coupled to one another under retention of sufficient substrate specificity. It has to be pointed out that the experimental finding of two distinct binding sites on either membrane side cannot be due to a mixed orientation of reconstituted carrier molecules, as was explained previously [15]. Nevertheless, the question of protein orientation in the liposomal membrane is of major importance when interpreting the results of kinetic analyses. There are several lines of evidence that the oriented reconstitution observed in the case of other carriers reconstituted by the applied method (19–21,30) also holds true for the dicarboxylate carrier: (i) Upon variation of substrate concentrations over a range that covered the  $K_m$  for both internal and external malate (or phosphate, respectively) activity data were obtained that in double reciprocal plots could be fitted by a single straight line showing that on the outside only binding sites of higher (lower) affinity were present as compared to the inside. (ii) The external  $K_m$  values were almost identical to those measured previously at the cytosolic side of mitochondria ( $K_m(\text{malate}) = 0.25 \text{ mM}$ ,  $K_m(\text{phosphate}) = 1.5 \text{ mM}$  [7]). (iii) Non-competitive inhibition due to the formation of an inactive carrier-phosphate-malate complex could only be found at the external but not at the internal membrane surface, as will be discussed below. A non-competitive behavior of malate and phosphate also was observed externally in experiments with mitochondria [7].

#### *Kinetic regulation of a four binding site sequential system*

The presence of two binding sites on either membrane side was indicated by the non-competitive interaction of dicarboxylates and phosphate with the carrier. Whereas on the outside this could be observed directly when malate and phosphate were present simultaneously [7,15], on the inside no inhibition was found. The non-competitive inhibition became evident

internally only when applying the substrate analogues butyl malonate and phenyl phosphate (Figs 1B and 2A). The common intersection point on the abscissa obtained in these experiments indicates that  $K_i = K_m$ , meaning that substrate and inhibitor can bind to the respective sites without mutual interference. However, both sites will only be occupied simultaneously, thus causing inhibition if binding is faster than translocation. This prerequisite obviously is fulfilled for external but not for internal substrate binding, unless the substrate analogues butyl malonate and phenyl phosphate were applied which were not transported by the dicarboxylate carrier (not shown).

In line with this model a non-catalytic complex of the carrier when saturated by both malate and phosphate could be found only at the external [15] but not at the internal membrane side (Fig. 3A). This means that cytosolic phosphate, which has to be imported into the mitochondrion, cannot be displaced competitively from its binding site by dicarboxylates. These, however, inhibit transport non-competitively when accumulating in the cytosol.

A different situation was encountered at the internal membrane side. Inhibition by the simultaneous presence of malate and phosphate did not occur (Fig. 3A). Instead, inhibition was observed if only malate or phosphate was present at very high concentrations (Fig. 4A). Since the intramitochondrial malate concentration is at or below 1 mM [31] and intramitochondrial phosphate does not exceed concentrations of about 11 mM [32], the inhibition at the internal side presumably is not relevant *in vivo*. On the other hand, the intramitochondrial malate concentration varies from values significantly below the  $K_m$  measured in our experiments up to values higher than the transport affinity, depending on the metabolic state [31,33]. Thus, it is reasonable to assume that the transfer of reducing equivalents from mitochondria to cytosol by the dicarboxylate carrier, which has to occur in particular in gluconeogenesis from pyruvate [34], may be regulated by the change in the mitochondrial malate concentration.

The inhibition of the reconstituted dicarboxylate carrier observed at high internal phosphate or dicarboxylate concentrations is most easily explained by binding of malate also to the phosphate site, or of phosphate also to the malate site, respectively. A second low-affinity dicarboxylate site was suggested as well by non-linear Dixon plots showing an exponential increase of inhibition of malate/malate exchange at internal butyl malonate concentrations above 1 mM (data not shown). These data therefore suggest that the dicarboxylate site has some affinity also for phosphate and, vice versa, the phosphate site also for dicarboxylates. A weak specificity overlap between the two sites may not be surprising. It should be emphasized that



the dicarboxylate carrier accepts a relatively broad spectrum of substrates. External sulphate or sulphite was transported by the dicarboxylate site but thiosulphate was a ligand of the phosphate site [12,15]. Transport inhibition at very high external substrate concentrations could not be investigated for technical reasons. So far only substrate binding was discussed. Translocation in the framework of the so-called gated-pore model [35–37] assumes a transmembrane channel (see Refs 38–40) that is gated in a ‘flip-flop’ manner. Gating is triggered by substrate binding to a site in the center of the channel, i.e., between the two gates. In the case of the dicarboxylate carrier two binding sites on each membrane side have to be accessible for the respective ligands without mutual interference. To match the ‘flip-flop’ gating model to the sequential mechanism, this demand for independent binding sites can only be fulfilled assuming the presence of two channels (per dimeric carrier molecule), one associated with two internal, the other with two external binding sites, which have a more superficial localization. A central active site in either channel may be occupied during translocation after transfer of one substrate molecule from a superficial binding site. This transfer then could be the decisive step for transport catalysis to proceed.

### Acknowledgements

This work was supported by the Ministero dell’Università e della Ricerca Scientifica e Tecnologica (MURST), the target project Biotechnology and Bioinstrumentation of Consiglio Nazionale delle Ricerche (CNR), the Deutsche Forschungsgemeinschaft (SFB189) and the Fonds der Chemischen Industrie.

### References

- Meijer, A.J. and Van Dam, K. (1981) in *Membrane Transport* (Bonting, S.L. and De Pont, J., eds), pp. 235–256, Elsevier, Amsterdam.
- Kramer, R. and Palmieri, F. (1992) in *Molecular Mechanisms in Bioenergetics* (Ernster, L., ed.), pp. 359–384, Elsevier, Amsterdam.
- Chappell, J.B. and Haarhoff, K.N. (1967) in *Biochemistry of Mitochondria* (Kaniuga, Z., Slater, E.C. and Wojtczak, L., eds), p. 75, Academic Press, London.
- Quagliariello, E., Palmieri, F., Prezioso, G. and Klingenberg, M. (1969) *FEBS Lett.* 4, 251–254.
- Palmieri, F., Quagliariello, E. and Klingenberg, M. (1970) *Eur. J. Biochem.* 17, 230–238.
- McGivan, J.D. and Klingenberg, M. (1971) *Eur. J. Biochem.* 20, 392–399.
- Palmieri, F., Prezioso, G., Quagliariello, E. and Klingenberg, M. (1971) *Eur. J. Biochem.* 22, 66–74.
- Papa, S., Lofrumento, N.E., Kanduc, D., Paradies, G. and Quagliariello, E. (1971) *Eur. J. Biochem.* 22, 134–143.
- Crompton, M., Palmieri, F., Capano, M. and Quagliariello, E. (1974) *Biochem. J.* 142, 127–137.
- Crompton, M., Palmieri, F., Capano, M. and Quagliariello, E. (1974) *FEBS Lett.* 46, 247–250.
- Quagliariello, E., Passarella, S. and Palmieri, F. (1974) in *Dynamics of energy-transducing membranes* (Ernster, L., Estabrook, A. and Slater, E.C., eds), pp. 483–495, Elsevier, Amsterdam.
- Crompton, M., Palmieri, F., Capano, M. and Quagliariello, E. (1975) *Biochem. J.* 146, 667–673.
- Bisaccia, F., Indiveri, C. and Palmieri, F. (1988) *Biochim. Biophys. Acta* 933, 229–240.
- Indiveri, C., Capobianco, L., Kramer, R. and Palmieri, F. (1989) *Biochim. Biophys. Acta* 977, 187–193.
- Indiveri, C., Dierks, T., Kramer, R. and Palmieri, F. (1989) *Biochim. Biophys. Acta* 977, 194–199.
- Sluse, F.E., Ranson, M. and Liébecq, C. (1972) *Eur. J. Biochem.* 25, 207–217.
- Dierks, T., Riemer, E. and Kramer, R. (1988) *Biochim. Biophys. Acta* 943, 231–244.
- Sluse, F.E., Sluse-Goffart, C.M. and Duyckaerts, C. (1989) in *Anion Carriers of Mitochondrial Membranes* (Azzi, A., Nalecz, K.A., Nalecz, M.J. and Wojtczak, L., eds), pp. 183–195, Springer, Berlin.
- Indiveri, C., Dierks, T., Kramer, R. and Palmieri, F. (1991) *Eur. J. Biochem.* 198, 339–347.
- Sluse, F.E., Evens, A., Dierks, T., Duyckaerts, C., Sluse-Goffart, C.M. and Kramer, R. (1991) *Biochim. Biophys. Acta* 1058, 329–338.
- Bisaccia, F., De Palma, A., Dierks, T., Kramer, R. and Palmieri, F. (1993) *Biochim. Biophys. Acta* 1042, 139–145.
- Bisaccia, F., Indiveri, C. and Palmieri, F. (1985) *Biochim. Biophys. Acta* 810, 362–369.
- Kramer, R. and Heberger, C. (1986) *Biochim. Biophys. Acta* 863, 289–296.
- Palmieri, F. and Klingenberg, M. (1979) *Methods Enzymol.* 56, 279–301.
- Kusov, Y.Y. and Kalinchuk, N.A. (1978) *Anal. Biochem.* 88, 256–262.
- Bisaccia, F. and Palmieri, F. (1984) *Biochim. Biophys. Acta* 766, 386–394.
- Palmieri, F. and Quagliariello, E. (1978) in *Bioenergetics at mitochondrial and cellular levels* (Wojtczak, J., Lenartowicz, E. and Zborowski, J., eds), pp. 5–38, Nencki Institute of Experimental Biology, Warsaw.
- Cleland, W.W. (1970) in *The Enzymes* (Boyer, P.D., ed.), Vol. 2, pp. 1–65, Academic Press, New York.
- Segel, I.H. (1975) *Enzyme Kinetics*, pp. 274–320, Wiley, New York.
- Klingenberg, M. and Winkler, E. (1986) *Methods Enzymol.* 127, 772–779.
- Soboll, S., Elbers, R., Scholz, R. and Heldt, H.W. (1980) *Biol. Chem. Hoppe-Seyler* 361, 69–76.
- Soboll, S., Scholz, R. and Heldt, H.W. (1978) *Eur. J. Biochem.* 87, 377–390.
- Soboll, S., Scholz, R., Freisl, M., Elbers, R. and Heldt, H.W. (1976) in *Use of Isolated Liver Cells and Kidney Tubules in Metabolic Studies* (Tager, J.M., Soling, H.D. and Williamson, J.R., eds), pp. 29–40, North-Holland, Amsterdam.
- Meijer, A.J. and Van Dam, K. (1974) *Biochim. Biophys. Acta* 346, 213–244.
- Klingenberg, M. (1976) in *The Enzymes of Biological Membranes*, Vol. 3 (Martonosi, A.N., ed.), pp. 383–438, Plenum, New York.
- Klingenberg, M. (1981) *Nature* 290, 449–454.
- Klingenberg, M. (1989) *Arch. Biochem. Biophys.* 270, 1–14.
- Dierks, T., Salentin, A., Heberger, C. and Kramer, R. (1990) *Biochim. Biophys. Acta* 1028, 268–280.
- Dierks, T., Salentin, A. and Kramer, R. (1990) *Biochim. Biophys. Acta* 1028, 281–288.
- Indiveri, C., Tonazzi, A., Dierks, T., Kramer, R. and Palmieri, F. (1992) *Biochim. Biophys. Acta* 1140, 53–58.